Simultaneous EMI Suppression of the Input and Output Terminals of a DC/DC Converter by Injecting Multiple Synthesized Cancellation Signals

Andreas Bendicks, Marvin Rübartsch, Stephan Frei
TU Dortmund University, On-board Systems Lab
Dortmund, Germany
andreas.bendicks@tu-dortmund.de

***Abstract*—Active cancellation of disturbances of power electronic systems is a common method in EMC. Most publications on this topic deal with the cancellation of either common or differential mode disturbances at either the input or the output terminals. In many systems, all disturbance modes of all terminals must be suppressed simultaneously. This is no trivial task since the different injectors for the anti-noise can affect each other. Therefore, a cancellation signal for the input terminals can worsen the noise at the output terminals, or vice versa. Additionally, due to mode conversion, common and differential mode can also interfere. In this work, synthesized cancellation signals are utilized that have already shown a very good performance in the suppression of periodic disturbances since complex transfer functions and delay times can be compensated. For the first time, a multi-port canceller is applied that injects synthesized cancellation signals to reduce the noise at four terminals simultaneously. The canceller enables a characterization of the system and an identification of the mutual coupling between the injectors. From this knowledge, the cancellation circuits can be designed purposefully. Furthermore, the mutual coupling can be respected in the calculation of the cancellation signals. A fundamental theory is described for DC/DC converters and applied to a 48 V/12 V converter in a measurement setup for conducted emissions according to the automotive EMC standard CISPR 25. The effectivity of the method is shown by measurements at artificial networks. The power losses of the cancellation system are estimated.**

Keywords—DC/DC Converter; EMI; Active Noise Suppression; Synthesized Signals; Multiple Terminals

I. INTRODUCTION

Power electronic DC/DC converters are often considerable sources of EMI. To comply with international standards (e.g. [1] in automotive), the EMI is commonly reduced by the application of passive filters or shields that may be bulky, heavy and expensive. Another strategy is the active cancellation of disturbing signals by a destructive interference between noise and anti-noise [2]. This strategy is applied commonly in acoustics and successively in EMC.

For EMC, active EMI filters have been introduced in [3], elaborated on in e.g. [4]-[6], and further generalized and analyzed in e.g. [7] and [8]. Like passive EMI filters, active filters are connected between the noise source and the sink. Already developed active filters can be classified as feedforward- or feedback-types. In feedforward active filters, the disturbances are measured at the noise source, processed and injected back into the system in direction of the noise sink to achieve a destructive interference between noise and anti-noise. Feedback active filters utilize a control loop to minimize the disturbances at the sink; here, the anti-noise is generated from the residual noise. As all analog or digital circuitry introduces an inevitable delay, the noise and anti-noise can never be exactly simultaneous. Hence, the achievable EMI reduction and the suppressible frequency range are limited for active filters as analyzed in [9]. To resolve the issue of a systematically delayed signal path, the cancellation signal can be artificially synthesized and applied in synchronicity with the disturbances [9], [10]. Remaining magnitude responses, phase-shifts and delays are compensated by the shape of the synthesized signal improving the cancellation's effectivity widely. This strategy performs especially well for periodic disturbances since the signal can be constructed from harmonic sine waves. So, it is well suited for the here considered DC/DC converter in its stationary operating mode, and it offers significant advantages over feedforward and feedback active filters. Therefore, this strategy is applied in this work.

Active filters have already been applied to DC/DC converters. There are investigations on the suppression of common (e.g. [8], [11], [12]) or differential (e.g. [13]-[15]) mode disturbances for either the input or the output of the converter. The cancellation by injecting synchronized and synthesized cancellation signals has yet only been shown for the differential mode disturbances at the input terminals of a DC/DC converter. Practical systems have multiple terminals, and the noise at all terminals must be suppressed simultaneously. This is no trivial task since the injectors can influence each other. E.g., the cancellation signal for the input can worsen the disturbances at the output, and vice versa. Additionally, due to mode conversion, the injectors for common or differential mode can affect each other mutually. These effects must be compensated to achieve a successful suppression of all terminals. The injection of synthesized and synchronized cancellation signals offers multiple advantages at this point. For this method, one central digital system can control all of the installed injectors. If the mutual interference is determined, the central cancellation control can adjust the signals of each injector to compensate this effect. Furthermore, the system is characterized as a byproduct. By evaluating the corresponding transfer functions, the cancellation system can be designed specifically for the application. As discussed later, there is much

design freedom for a central cancellation system with scattered injectors.

In this work, a DC/DC converter (e.g. for automotive applications) is suppressed in regard to all of its disturbance modes and terminals for frequencies of up to 30 MHz. To do so, a specialized theory is developed. In this theory, the system is characterized and the necessary cancellation signals are determined mathematically. Due to the comprehensive characterization, all mutual couplings can be compensated. Afterward, this theory is applied to a DC/DC converter in a laboratory setup. The application, the test setup and the designed cancellation system are depicted. The implemented procedure for characterizing the system and calculating the cancellation signals is explained. Emission measurement results are shown and the power consumption of the cancellation system is estimated. A conclusion and an outlook close the work.

II. Theory

In this chapter, a fundamental theory is given for a simultaneous cancellation of the input and output terminals of a generic DC/DC converter. At first, the overall system is introduced and mathematically described. Afterward, the necessary cancellation signals are calculated. Requirements for a successful calculation are discussed. Last, three variants for implementation are depicted.

A. Mathematical Description of the System

In this section, the overall system (Figure 1) is described to allow an efficient calculation of the necessary cancellation signals. The considered DC/DC converter has four terminals; one for each DC+ and DC- at input and output, respectively. The converter is supplied by the DC voltage source V_{supply} between the input terminals. At the output terminals, the converter supplies the voltage V_{load} to a load. In regard to [1], the conducted emissions are measured by artificial networks (AN) that are connected to the input and output terminals of the device under test (DUT). The ANs represent a defined termination for the DUT's disturbances and they provide ports for standardized measurement. To suppress the disturbances, injectors are installed between the noise source (switching DC/DC converter) and the noise victims (ANs). Since four terminals must be suppressed, four cancellation signals are necessary. The here defined DUT comprises the DC/DC converter and the injectors.

If the converter uses ground as DC-, there are only disturbances between DC+ and ground. Therefore, only two artificial networks are necessary; one for the input and one for the output, both at DC+. Also, only two cancellation sources are needed in this case.

1) Noise

The switching of the DC/DC converter generates noise (symbolized by a voltage source $V_{\mathrm{noise}}(f)$) that propagates through the system. The noise at the input and output terminals is denoted by $\vec{V}_{\mathrm{noise}}^{\mathrm{in/out}}(f)$:

$$\vec{V}_{\mathrm{noise}}^{\mathrm{in/out}}(f) = \begin{pmatrix} V_{\mathrm{noise}}^{\mathrm{in,DC+}}(f) \\ V_{\mathrm{noise}}^{\mathrm{in,DC-}}(f) \\ V_{\mathrm{noise}}^{\mathrm{out,DC+}}(f) \\ V_{\mathrm{noise}}^{\mathrm{out,DC-}}(f) \end{pmatrix}$$

2) Anti-Noise

In general, an arbitrary injector can be applied for the anti-noise. It is possible to utilize voltage (considered here) or current sources, or a mix of both. The coupling is usually done with a capacitor or an inductive transducer. It is possible to suppress common and differential mode, or each line voltage to ground individually. The latter approach is applied in this paper. Additional components for decoupling have to be added if there are, e.g., current paths in the system that can short the injected signals. The generated anti-noise is denoted by the vector $\vec{V}_{\mathrm{anti}}(f)$:

$$\vec{V}_{\mathrm{anti}}(f) = \begin{pmatrix} V_{\mathrm{anti},1}(f) \\ V_{\mathrm{anti},2}(f) \\ V_{\mathrm{anti},3}(f) \\ V_{\mathrm{anti},4}(f) \end{pmatrix}$$

Like the noise, also the anti-noise propagates through the system. The resulting anti-noise at the input and output terminals is denoted by $\vec{V}_{\mathrm{anti}}^{\mathrm{in/out}}(f)$:

$$\vec{V}_{\mathrm{anti}}^{\mathrm{in/out}}(f) = \begin{pmatrix} V_{\mathrm{anti}}^{\mathrm{in,DC+}}(f) \\ V_{\mathrm{anti}}^{\mathrm{in,DC-}}(f) \\ V_{\mathrm{anti}}^{\mathrm{out,DC+}}(f) \\ V_{\mathrm{anti}}^{\mathrm{out,DC-}}(f) \end{pmatrix}$$

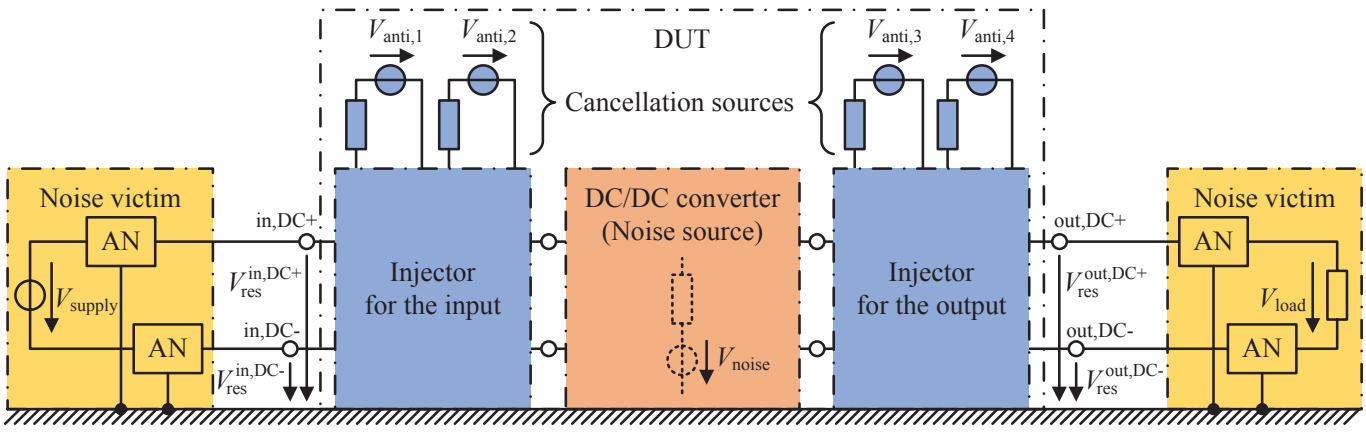

Figure 1: Model of the overall system

The relationship between the generated anti-noise $\vec{V}_{\mathrm{anti}}(f)$ and the resulting anti-noise at the inputs and outputs $\vec{V}_{\mathrm{anti}}^{\mathrm{in/out}}(f)$ can be described by the 4×4 transfer matrix $H_{\mathrm{anti}}(f)$:

$$\vec{V}_{\mathrm{anti}}^{\mathrm{in/out}} = \boldsymbol{H}_{\mathrm{anti}} \cdot \vec{V}_{\mathrm{anti}} \tag{1}$$

3) Residual Disturbances

The residual disturbances at the input and output terminals are denoted by $\vec{V}_{\mathrm{res}}^{\mathrm{in/out}}(f)$:

$$\vec{V}_{\mathrm{res}}^{\mathrm{in/out}}(f) = \begin{pmatrix} V_{\mathrm{res}}^{\mathrm{in,DC+}}(f) \\ V_{\mathrm{res}}^{\mathrm{in,DC-}}(f) \\ V_{\mathrm{res}}^{\mathrm{out,DC+}}(f) \\ V_{\mathrm{res}}^{\mathrm{out,DC-}}(f) \end{pmatrix}$$

These residual disturbances are described by the superposition of noise $\vec{V}_{\mathrm{noise}}^{\mathrm{in/out}}(f)$ and anti-noise $\vec{V}_{\mathrm{anti}}^{\mathrm{in/out}}(f)$:

$$\vec{V}_{\mathrm{res}}^{\mathrm{in/out}} = \vec{V}_{\mathrm{noise}}^{\mathrm{in/out}} + \vec{V}_{\mathrm{anti}}^{\mathrm{in/out}} \tag{2}$$

The disturbances picked up by the ANs are basically the residual disturbances of the input and output terminals.

B. Calculation of the Cancellation Signals

From the mathematical description found above, the necessary cancellation signals can be determined. By combining (1) and (2), (3) results.

$$\vec{V}_{\mathrm{res}}^{\mathrm{in/out}} = \vec{V}_{\mathrm{noise}}^{\mathrm{in/out}} + \boldsymbol{H}_{\mathrm{anti}} \cdot \vec{V}_{\mathrm{anti}} \tag{3}$$

The condition for a complete cancellation at the input and output terminals is formulated by (4).

$$\vec{V}_{\mathrm{res}}^{\mathrm{in/out}} = \vec{V}_{\mathrm{noise}}^{\mathrm{in/out}} + \boldsymbol{H}_{\mathrm{anti}} \cdot \vec{V}_{\mathrm{anti}} \; != \vec{0} \tag{4}$$

To find the appropriate complex amplitudes for cancellation, (4) can be solved to:

$$\vec{V}_{\mathrm{anti}} = -\boldsymbol{H}_{\mathrm{anti}}^{-1} \cdot \vec{V}_{\mathrm{noise}}^{\mathrm{in/out}} \tag{5}$$

Obviously, $\boldsymbol{H}_{\mathrm{anti}}$ must be regular to do so. This requirement is discussed in II.C. From the complex amplitudes $\vec{V}_{\mathrm{anti}}(f)$, the cancellation signals can be synthesized. By applying these signals to the cancelling sources, all disturbances at the input and output terminals and all disturbances at the noise victims are suppressed. Note that all mutual interferences between the cancelling sources and the input and output terminals are respected in $\boldsymbol{H}_{\mathrm{anti}}$. So, the mutual interference is intrinsically compensated in $\vec{V}_{\mathrm{anti}}(f)$.

C. Requirements for the Transfer Matrix

The transfer matrix $\boldsymbol{H}_{\mathrm{anti}}$ must be regular so that the inverse $\boldsymbol{H}_{\mathrm{anti}}^{-1}$ exists and equation (5) can be solved analytically. There are two necessary considerations.

First, the rank of the matrix must be full since the matrix is not invertible otherwise. For a full rank, all injectors and terminals must be linearly independent, respectively. In general, there may be a linear dependency if two or more injectors inject e.g. a current into the same node. This may be obvious if there is a galvanic connection. In some cases, it is not that obvious if, e.g., large capacitances behave like shorts at high frequencies. The same is true for the input and output terminals. To resolve this issue, it is possible to decouple the nodes or branches by additional circuitry in the injector's circuit.

Second, the matrix must be well conditioned so that the inverse can be calculated precisely. Noteworthy, the condition becomes worse the closer the matrix gets to a reduced rank. This may indicate, e.g., a mutual coupling of injectors. So, it is encouraged to ensure a strong linear independency between the injectors and the output terminals.

D. Variants for Implementation

In this section, some possibilities for implementation are discussed that depends on the knowledge of the system.

In the first scenario, the system is completely known. Hence, the disturbances at the input and output terminals $\vec{V}_{\mathrm{noise}}^{\mathrm{in/out}}$, the transfer matrix $\boldsymbol{H}_{\mathrm{anti}}$ and the necessary cancellation signals $\vec{V}_{\mathrm{anti}}$ can easily be calculated.

In the second scenario, the system must be characterized. To do so, sensors can be placed at the output terminals. Now, the disturbances at the input and output terminals $\vec{V}_{\mathrm{noise}}^{\mathrm{in/out}}$ can be measured and the transfer matrix $\boldsymbol{H}_{\mathrm{anti}}$ can be determined. From (5), the necessary cancellation signal $\vec{V}_{\mathrm{anti}}$ can be calculated and synthesized. The characterization and generation of appropriate signals (teach-in) can be done for all relevant operating modes and setups of the system. An interpolation between, e.g., operating modes can help to reduce the number of measurements. After this procedure, the noise sensors can be removed. Note that the removal of the sensors can change the transfer functions and disturbances of the system. Due to this effect, the previously found cancellation signals may differ from the ones now necessary. To avoid this issue, sensors can be chosen that influence the transfer functions as little as possible, or the impedance of the sensors can be substituted after removal. In III, this strategy is demonstrated for one operating mode of the DC/DC converter (but the sensors are not uninstalled after teach-in). In [10], a similar method has been demonstrated utilizing an EMI receiver for teach-in. The main difference is in the sensing circuit; in [10], the signal has been optimized for a noise sink (an artificial network) and not for an additionally installed sensor.

In the third scenario, the system changes during operation or there is too much data to collect in the prior teach-in phase. To resolve this problem, sensors can be installed permanently at the input and output terminals. Now, the cancellation system can adapt itself continuously to the changing disturbances and setups. In [9], a self-adapting cancellation prototype has been realized that consists of an FPGA, an ADC and a DAC.

III. Demonstration

In this chapter, the theory of II is applied to a laboratory setup. At first, the application is introduced. Afterward, the test setup and the cancellation equipment are depicted. For this setup, suitable injectors and sensors are designed. Then, the characterization procedure is described, and the necessary cancellation signals are calculated. The performance of the method is evaluated by measurements and the power consumption of the cancellation system is estimated.

A. Application

For demonstration, a GaN-transistor evaluation board GS61008P-EVBHF is used as DC/DC converter that steps an input voltage of 48 V down to 12 V. The switching frequency is set to $f_0 = 1$ MHz. Since the duty cycle is kept constant, there are stable disturbing harmonics with a spacing of f_0. The control signal for the DC/DC converter is generated by an arbitrary waveform generator (AWG). To galvanically isolate the control signal from ground, a digital isolator is applied.

B. Test Setup and Cancellation Equipment

The test setup referring to [1] is depicted in Figure 2. The overall setup is placed on a copper table as ground plane. The DUT consists of the DC/DC converter and the cancellation system that is presented in the following sections. For demonstration, the converter is galvanically isolated from the ground plane. So, there are common and differential mode disturbances for both the input and the output. In other words, there is noise on all four lines that must be suppressed. For measurement, all lines are terminated by an individual artificial network. So, the disturbing voltages of the lines are picked up against the ground plane. The disturbances are measured by an EMI receiver. The 48 V input voltage is provided by a power supply. The load for the 12 V output is a 1 Ω resistor. So, there is a transfer power of approximately 144 W.

Three synchronized AWGs (Tektronix AFG3000 series) with two output channels each are used to control the DC/DC converter and to inject four cancellation signals into the system. For feedback measurement, an oscilloscope (LeCroy HDO6104A) is used. A PC with Matlab is used to calculate the necessary cancellation signals and to control the cancellation equipment via Ethernet. In practical realizations, this equipment can be substituted by low-cost mixed-signal integrated circuits.

For demonstration, the frequency range up to 30 MHz shall be suppressed actively. Due to the switching frequency of 1 MHz, there are 30 harmonics inside of the considered frequency range that must be suppressed. Peak and average emissions are mostly the same since the disturbances are stationary. Here, the average emissions are measured and depicted. According to [1], a resolution bandwidth of 9 kHz is applied.

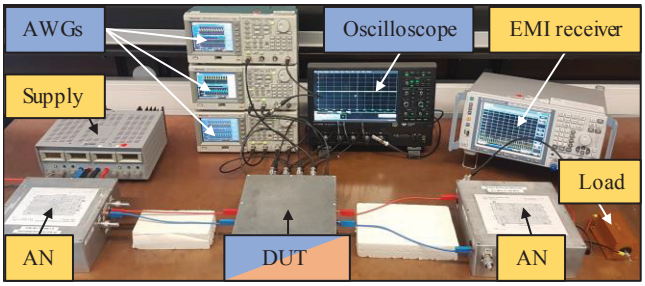

Figure 2: Photograph of the test setup

C. Design of the Cancellation System

A photograph and the schematic of the DUT are depicted in Figure 3 and Figure 4, respectively. The four input and output terminals are galvanically connected to the converter (noise source). The switching node is capacitively coupled to the ground plane.

1) Injectors

For cancellation, capacitively coupled injectors have been chosen. The coupling is done by 100 nF capacitors and the signals $\vec{V}_{\text{anti}}$ are generated by the AWGs. Without decoupling inductors, significant portions of the injected currents flow into the

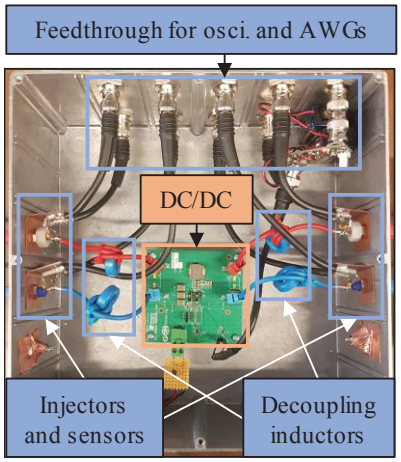

Figure 3: Photograph of the DUT

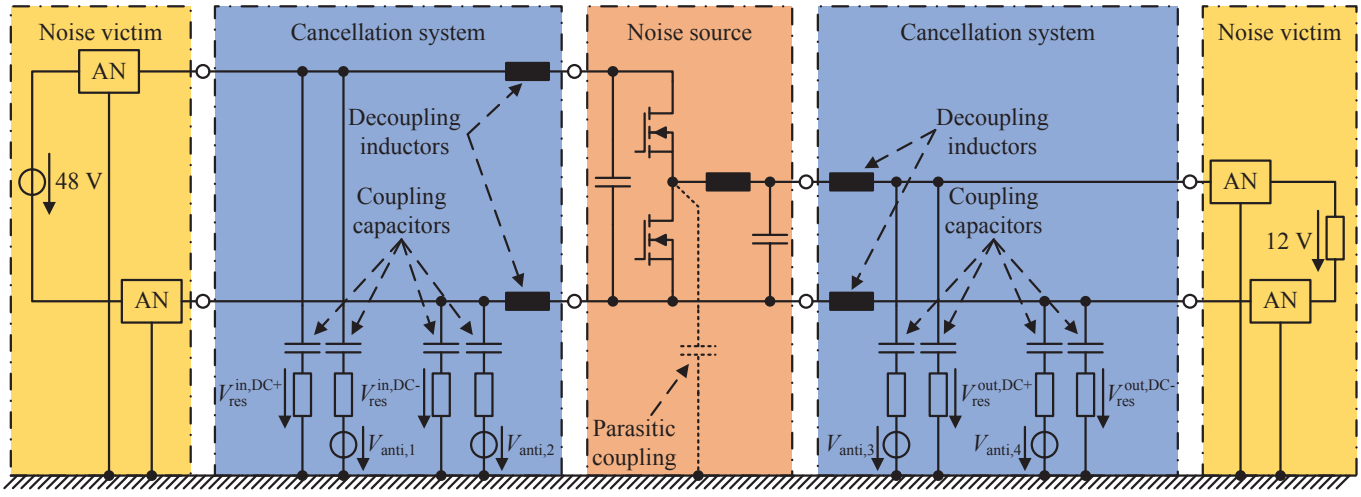

Figure 4: Schematic of the DUT

converter and not to the actual noise sinks where the cancellation should take place. Therefore, the cancellation sources must provide high voltages to inject the necessary current into the sinks. Furthermore, the injectors are strongly coupled. Therefore, the condition number of the matrix $\boldsymbol{H}_{\mathrm{anti}}$ is large, and the precision of the results of (5) is limited. To resolve this issue, toroidal ferrites are installed for decoupling. By doing so, the necessary cancellation voltages are reduced and the condition of the matrix is improved. To utilize the full resolution of the AWG, 10 dB attenuators are added between channels of the AWGs and the injectors. Therefore, the series resistances of the cancellation sources depicted in Figure 4 consist of the internal AWG resistance of 50 Ω and the attenuator.

2) Sensors

For feedback measurement, capacitive sensors (with 100 nF capacitors) are applied to each line. Therefore, the sensors directly measure the residual disturbances at the input and output terminals $\vec{V}_{\mathrm{res}}^{\mathrm{in/out}}$ that comprise $V_{\mathrm{res}}^{\mathrm{in,DC+}}$, $V_{\mathrm{res}}^{\mathrm{in,DC-}}$, $V_{\mathrm{res}}^{\mathrm{out,DC+}}$ and $V_{\mathrm{res}}^{\mathrm{out,DC-}}$. The measurement is done by an oscilloscope. To improve the precision, the measurement bandwidth is limited to the considered frequency range by external low-pass filters. For impedance matching, 3 dB attenuators are installed between the sensor and the low-pass filter. So, there is basically a termination of 50 Ω in regard to the schematic in Figure 4.

D. Characterization and Calculation of Cancellation Signals

As stated before, a PC with Matlab is used to determine the necessary cancellation signals. Here, the program sequence is depicted. There are basically three steps.

First, the noise of the DC/DC converter at the sensors $\vec{V}_{\mathrm{noise}}^{\mathrm{in/out}}$ is determined. To do so, the cancellation signals are turned off ($\vec{v}_{\mathrm{anti,test}}(t) \equiv \vec{0}$) and the DC/DC converter is turned on. The disturbances $\vec{v}_{\mathrm{res,meas.}}^{\mathrm{in/out}}(t)$ are measured by the oscilloscope. The data is sent to the PC and the harmonics $\vec{V}_{\mathrm{res,meas.}}^{\mathrm{in/out}}(kf_0)$ are determined by a fast Fourier transform (FFT). Due to $\vec{V}_{\mathrm{anti,test}}(kf_0) \equiv \vec{0}$, $\vec{V}_{\mathrm{noise}}^{\mathrm{in/out}}(kf_0) = \vec{V}_{\mathrm{res,meas.}}^{\mathrm{in/out}}(kf_0)$ follows from (3).

Second, the transfer matrix $\boldsymbol{H}_{\mathrm{anti}}(kf_0)$ is determined. Obviously, the transfer functions must be found as precisely as possible. Since the DC voltage and current of the converter influence the transfer functions, the characterization is done with the DC/DC converter activated. The transfer matrix (with its 16 transfer functions) is determined by test measurements. Test signals $\vec{v}_{\mathrm{anti,test}}(t)$ can be synthesized from arbitrary harmonics $\vec{V}_{\mathrm{anti,test}}(kf_0)$ with the same frequencies as the disturbances. Since the DC/DC converter is turned on, the sensors measure not only the influence of the test signals $\vec{V}_{\mathrm{anti,test}}^{\mathrm{in/out}}(kf_0)$, but also the (previously determined) disturbances $\vec{V}_{\mathrm{noise,known}}^{\mathrm{in/out}}(kf_0)$. The relationship of (6) results from (3).

$$\vec{V}_{\mathrm{res,meas.}}^{\mathrm{in/out}} - \vec{V}_{\mathrm{noise,known}}^{\mathrm{in/out}} = \boldsymbol{H}_{\mathrm{anti}} \cdot \vec{V}_{\mathrm{anti,test}} \qquad (6)$$

Since there is no easy way to determine the complete matrix $\boldsymbol{H}_{\mathrm{anti}}(kf_0)$ at once, the entries (transfer functions) are determined individually by applying the test signal to only one injector at a time. So, the influence of the injectors to the different sensors is systematically included which directly represents the mutual coupling of the injectors.

Thirdly, the cancelling harmonics $\vec{V}_{\mathrm{anti}}(kf_0)$ are calculated from $\boldsymbol{H}_{\mathrm{anti,known}}(kf_0)$ and $\vec{V}_{\mathrm{noise,known}}^{\mathrm{in/out}}(kf_0)$ by (5). From these harmonics, the cancellation signals $\vec{v}_{\mathrm{anti}}(t)$ are synthesized and applied to the system. Note that the mutual interferences between the injectors are respected in the transfer matrix $\boldsymbol{H}_{\mathrm{anti,known}}(kf_0)$ and compensated by solving (5).

To improve the result, multiple iterations can be done. In this case, the residual disturbances are measured and additional cancellation signals are determined to suppress the disturbances even further. Then, the old cancellation signals are superposed with the new ones to generate the updated cancellation signals.

E. Measurement Results

The measurement results of the EMI receiver for all four ANs are depicted in Figure 5. All disturbing harmonics are evenly suppressed to approximately 40 dBµV. This limit is related to the quantization noise level of the cancellation equipment. The fundamental waves are suppressed by 50 dB on average. Even the harmonics at 30 MHz are suppressed by 40 dB

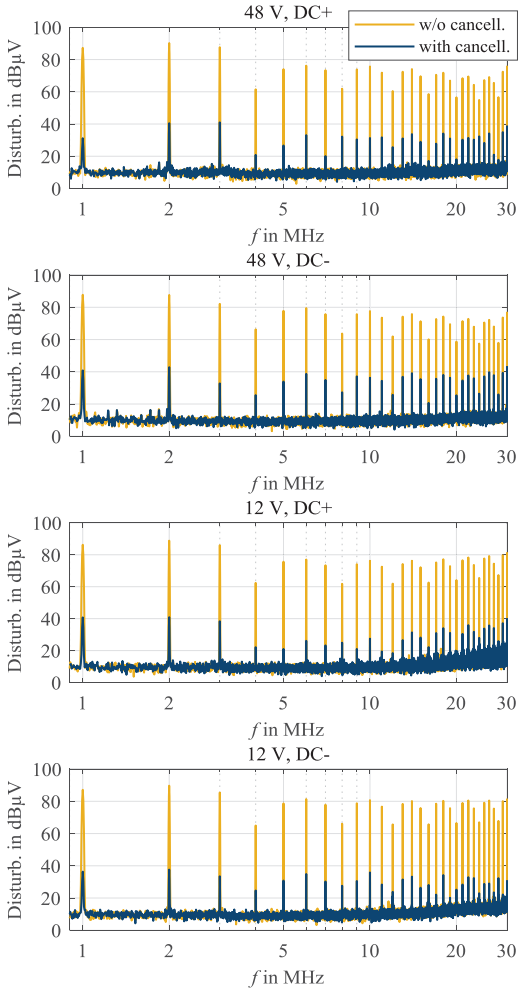

Figure 5: Measured disturbances at the artificial networks with and without active cancellation

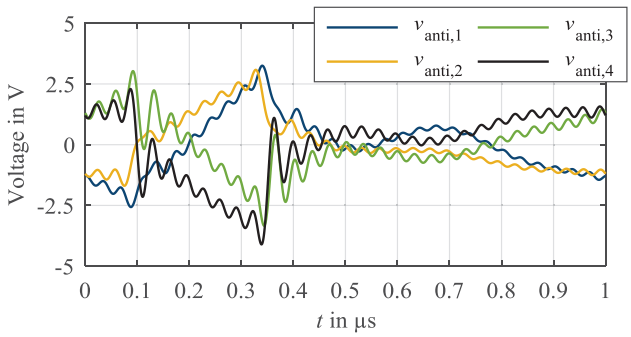

Figure 6: Found cancellation signals for all four injectors over one switching period

on average. Therefore, the method proves to be very effective in the considered frequency range.

F. Power Consumption

To estimate the power consumption of the cancellation system, the determined cancellation signals $\vec{v}_{\text{anti}}(t)$ (Figure 6) are evaluated. The RMS voltages of the signals are calculated to $\vec{V}_{\text{anti,rms}} \approx [1.2\ \text{V}, 1.1\ \text{V}, 1.1\ \text{V}, 1.4\ \text{V}]^{\text{T}}$. The total power consumption of the cancellation sources $P_{\text{anti,total}}$ can be estimated by (7).

$$P_{\text{anti,total}} = \frac{\vec{V}_{\text{anti,rms}}^{\text{T}} \cdot \vec{V}_{\text{anti,rms}}}{R_{\text{AWG}} + R_{\text{termination}}} \tag{7}$$

The AWG's internal resistance of 50 Ω is denoted by R_{AWG}. Due to the 10 dB attenuator, there is an impedance matching for the AWG, and the termination impedance $R_{\text{termination}}$ can be approximated to 50 Ω. From this data, the total power consumption can be calculated to $P_{\text{anti,total}} \approx 58\ \text{mW}$. This value is only approximately 0.04 % of the transfer power of 144 W.

IV. Conclusion and Outlook

In this work, synthesized cancellation signals have been utilized for the first time to simultaneously suppress the disturbances of multiple terminals of a power electronic system. Here, a DC/DC converter has been suppressed in regard to its two input and two output terminals. From a comprehensive theory, the mutual coupling of the injectors has been identified. Suitable cancellation signals have been found by an appropriate calculation that intrinsically takes the mutual coupling into account. General possibilities, requirements and variants for implementation have been discussed. A suitable cancellation system has been designed for the considered DC/DC converter in a standard EMC test setup. Measurements have shown that the noise has been reduced by about 50 dB at 1 MHz and 40 dB at 30 MHz for all artificial networks of the test setup. Furthermore, it has been shown that the power consumption of the cancellation system is negligible compared to the transfer power of the DC/DC converter. All in all, the injection of multiple synthesized cancellation signals proves to be a very effective method to suppress the disturbances of multiple terminals of a DC/DC converter. Here, laboratory equipment has been used to demonstrate the method. In practical realizations, specialized mixed-signal integrated circuits can be utilized at low costs.

Currently, the presented method is being investigated further to determine the limits of the cancellation system. Additionally, the theory is being developed further to be applicable on arbitrary systems.

V. Acknowledgment

This work was partially supported by the company Leopold Kostal GmbH & Co. KG. The authors gratefully acknowledge the cooperation and express special thanks to Norbert Hees and Marc Wiegand for their assistance and especially the very valuable discussions.

References

[1] "CISPR 25 – *Vehicles, boats and internal combustion engines – Radio disturbance characteristics – Limits and methods of measurement for the protection of on-board receivers*," Ed.4.0, 2015.

[2] P. Lueg, "Process of silencing sound oscillations," U.S. Patent 2 043 416, Jun. 9, 1936.

[3] J. Walker, "Designing practical and effective active EMI filters," in Proc. *Powercon 11 Conf.*, Dallas, Texas, USA, Apr. 1984, Paper I-3.

[4] L. E. LaWhite, M. F. Schlecht, "Design of active ripple filters for power circuits operating in the 1-10 MHz range," *IEEE Trans. Power Electron.*, vol. 3, no. 3, pp. 310-317, Jul. 1988.

[5] L. E. LaWhite, M. F. Schlecht, "Active filters for 1 MHz power circuits with strict input/output requirements," in *17th Annual IEEE Power Electronics Specialists Conf.*, Vancouver, Canada, 23-27 Jun. 1986, pp. 255-263.

[6] T. Farkas, M. F. Schlecht, "Viability of active EMI filters for utility applications," *IEEE Trans. Power Electron.*, vol. 9, no. 3, pp. 328-337, May 1994.

[7] N. K. Poon, J. C. P. Liu, C. K. Tse, M. H. Pong, "Techniques for input ripple current cancellation: classification and implementation," *IEEE Trans. Power Electron.*, vol. 15, no. 6, pp. 1144-1152, Nov. 2000.

[8] Y.-C. Son, S.-K. Sul, "Generalization of active filters for EMI reduction and harmonics compensation," *IEEE Trans. Ind. Appl.*, vol. 42, no. 2, pp. 545-551, Mar./Apr. 2006.

[9] A. Bendicks, T. Dörlemann, S. Frei, N. Hees, M. Wiegand, "Active EMI Reduction of Stationary Clocked Systems by Adapted Harmonics Cancellation," *IEEE Trans. Electromagn. Compat.*, Early Access, pp. 1-9, Aug. 2018.

[10] A. Bendicks, S. Frei, "Broadband Noise Suppression of Stationary Clocked DC/DC Converters by Injecting Synthesized and Synchronized Cancellation Signals," *IEEE Trans. Power Electron.*, Early Access, pp. 1-1, Jan. 2019.

[11] D. Shin, S. Kim, G. Jeong, J. Park, J. Park, K. J. Han, J. Kim, "Analysis and design guide of active EMI filter in a compact package for reduction of common-mode conducted emissions," *IEEE Trans. Electromagn. Compat.*, vol. 57, no. 4, pp. 660-671, Aug. 2015.

[12] D. Shin, S. Jeong, J. Kim, "Quantified design guidelines of a compact transformerless active EMI filter for performance, stability, and high voltage immunity," *IEEE Trans. Power Electron.,* vol. 33, no. 8, pp. 6723-6737, Aug. 2018.

[13] M. Zhu, D.J. Perreault, V. Caliskan, T.C. Neugebauer, S. Guttowski, J.G. Kassakian, "Design and evaluation of Feedforward Active ripple filters", *IEEE Trans. Power Electron.*, vol. 20, no. 2, Mar. 2005.

[14] R. Goswami, S. Wang, "Modeling and stability analysis of active differential-mode EMI filters for ac/dc power converters," *IEEE Trans. Power Electron.*, vol. 33, no. 12, pp. 10277-10291, Dec. 2018.

[15] R. Goswami, S. Wang, E. Solodovnik, K. Karimi, "Differential mode active EMI filter design for a boost power factor correction (PFC) ac/dc converter," *IEEE Journal of Emerging and Selected Topics in Power Electronics*, vol. 7, no. 1, pp. 576-590, Mar. 2019.